Bioorganic & Medicinal Chemistry Letters 22 (2012) 4396–4403

Contents lists available at SciVerse ScienceDirect

Bioorganic & Medicinal Chemistry Letters

journal homepage: www.elsevier.com/locate/bmcl

Fragment-based discovery of hydroxy-indazole-carboxamides as novel small molecule inhibitors of Hsp90

Hans-Peter Buchstaller *, Hans-Michael Eggenweiler, Christian Sirrenberg, Ulrich Grädler, Djordje Musil, Edmund Hoppe, Astrid Zimmermann, Harry Schwartz, Joachim März, Jörg Bomke, Ansgar Wegener, Michael Wolf

Merck Serono Research, Merck KGaA, Frankfurter Straße 250, D-64293 Darmstadt, Germany

ARTICLE INFO

Article history:
Received 2 April 2012
Revised 26 April 2012
Accepted 29 April 2012
Available online 5 May 2012

Dedicated to Professor Christian R. Noe on the occasion of his 65th birthday

Keywords:
Hsp90
Heat shock protein 90
Anti-cancer drug
Fragments
Indazoles
Docking
X-ray structure

ABSTRACT

Inhibitors of the Hsp90 molecular chaperone are showing considerable promise as potential molecular therapeutic agents for the treatment of cancer. Here we describe the identification of novel small molecular weight inhibitors of Hsp90 using a fragment based approach. Fragments were selected by docking, tested in a biochemical assay and the confirmed hits were crystallized. Information gained from X-ray structures of these fragments and other chemotypes was used to drive the fragment evolution process. Optimization of these high μM binders resulted in 3-benzylindazole derivatives with significantly improved affinity and anti-proliferative effects in different human cancer cell lines.

Molecular chaperones are proteins, which play a key role in the conformational maturation, stability and function of other client protein substrates within the cell.[1,2] Many of the client proteins of Heat shock protein 90 (Hsp90),[3–6] which are involved in signal transduction, cell cycle regulation and apoptosis, are well known oncogenes and are often deregulated (over-expressed and mutated) in tumor cells, and this dysregulation of pathways involving these proteins are commonly associated with cancer pathology.[7] The association of Hsp90 with these client proteins maintains their ability to function in the deregulated state. Therefore, Hsp90 inhibitors target tumor growth by multiple parallel mechanisms. Hsp90 has attracted considerable interest as a therapeutic target for anticancer drugs since it was shown that both geldanamycin[8] and radicicol[9] are able to inhibit Hsp90 function by binding to an ATP binding pocket in the N-terminal domain of the protein. Based on encouraging preclinical data several derivatives of these natural product inhibitors like 17-AAG, 17-DMAG and the prodrug of 17-AAG, IPI-504 entered clinical studies.[10] However, these compounds have several potential limitations, including poor solubility, limited bioavailability and hepatotoxicity. These issues have led to significant efforts to identify small-molecule inhibitors. Indeed, several compounds of different chemical classes have been disclosed so far, like ganetespib (STA-9090),[11] NVP-AUY922,[12] AT-13387,[13] Debio-0932 (CUDC-305)[14] or PU-H71[15] which have entered trials in different phases of clinical development (Fig. 1). A comprehensive overview has been published recently.[16]

Finding novel compounds as starting points for optimization is a major challenge in drug discovery research. Fragment-based approaches have rapidly become a proven technique to identify such starting points in a variety of research programs.[17] Furthermore, the optimization of fragment-like hits using structural information from protein X-ray crystallography has been established as a valuable strategy in the search for new drug molecules of various targets including Hsp90.[18] Herein, we describe the identification of low affinity indazoles and their optimization to potent inhibitors of the N-terminal ATP binding site of Hsp90.

A subset of about 64,000 compounds was preselected from our compound library by filtering with calculated fragment-like properties in adaption to the Astex 'rule of three' (e.g., MW <300).[19] This subset was used for virtual screening by docking in the ATPase binding site of Hsp90. The analysis of the X-ray structures of Hsp90 in complex with reference compounds (phenole and purine

* Corresponding author. Tel.: +49 6151724092; fax: +49 6151723129.
E-mail address: hans-peter.buchstaller@merckgroup.com (H.-P. Buchstaller).

0960-894X/$ - see front matter © 2012 Elsevier Ltd. All rights reserved.
http://dx.doi.org/10.1016/j.bmcl.2012.04.121

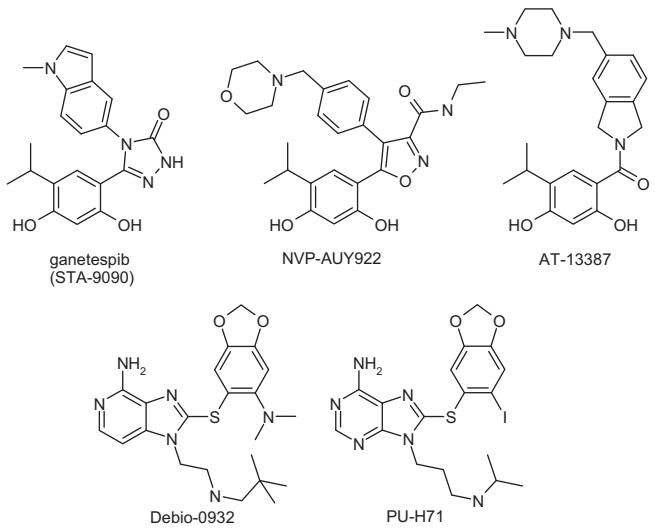

Figure 1. Selected structures of Hsp90 inhibitors in clinical trials.

derivatives) published at the time, when our virtual screening campaign was conducted, revealed crucial interactions within the ATP-site.[20,21] These interactions include hydrogen bonds of the phenolic OH-group and purine N-atoms to Asp93 and an adjacent conserved water-molecule (Fig. 2). The assigned hydrogen bond network of the phenolic OH-group in the Hsp90-complex suggested a donor contact to Asp93 and an acceptor interaction to the interstitial water molecule. Similarly, the purine amino group forms an H-bond donor contact to Asp93 and the N1-atom an acceptor contact to the conserved water-molecule. A large induced fit characterized by the transition of an open, 'apo-like' form as in the geldanamycin complex to a helical form upon binding of purine derivatives was observed in the rear ATP binding site of Hsp90.[22,23] This transition results in the presence of a large lipophilic pocket formed by the side chains of Met98, Leu107, Phe138, Tyr139, Val150 and Trp162 in the helical form. As demonstrated for purine analogs, the optimization of hydrophobic interactions within this lipophilic pocket has resulted in Hsp90 inhibitors with significant biochemical and cellular potency.[24] Consequently, we used a representative structure of the helical form (PDB code 1UYF) as rigid protein model for docking in order to also identify fragments potentially binding into this lipophilic pocket.

The composite inhibitor interactions served as pharmacophore constraints (Fig. 2) for the subsequent docking of a preselected subset of ~64,000 compounds from our corporate library using the program FlexX.[25] The pharmacophore contraints (see Supplementary data) were used as filters to select only fragments with suitable H-bonds to either Asp93 or the conserved water molecule in addition to potential hydrophobic contacts within the lipophilic pocket of the helical form which resulted in 3810 hits. These hits were ranked by a combination of two alternative docking scores (FlexX- and PLP-scoring functions), clustered by chemical substructures and the docking poses of top scored hits from each cluster were finally visually inspected. A subset of 96 fragments was finally selected for testing in a Hsp90 binding assay[26] revealing five hits with an IC_{50}-value below 100 μM (5% hit rate). Three of the hits were structurally similar, low molecular weight indazoles and the remaining two hits contained an aminopyrimidine or quinazoline moiety (Fig. 3a). The binding mode of all hits could be elucidated by X-ray crystallography using the ATPase domain of human Hsp90. A superimposition of the crystal structures revealed, that fragments III and V bind to the helical protein form with their bulky hydrophobic substituents (cyclohexyl and *p*-chlorophenyl respectively) oriented into the same lipophilic pocket as the substituted phenyl ring of Hsp90-purine complexes (e.g., as in PDB code 1UYF). In contrast, the three other fragments I, II and VI bind to the open Hsp90 conformation as present in the geldanamycin complex (Fig. 3b). Interestingly, X-ray structures confirmed that the hydroxy-indazoles bind in two reversed orientations in contact with Asp93 as predicted by our pharmacophore docking protocol (Figs. 4 and 5). Fragment II interacts via H-bonds of both indazole N-atoms to Asp93 and the conserved water molecule, while an identical interaction pattern is found for the phenolic OH-group of fragment III. The reversed orientation might be influenced by the substitution pattern of the hydroxindazole core as the cyclohexyl ring of fragment III is bound in the lipophilic

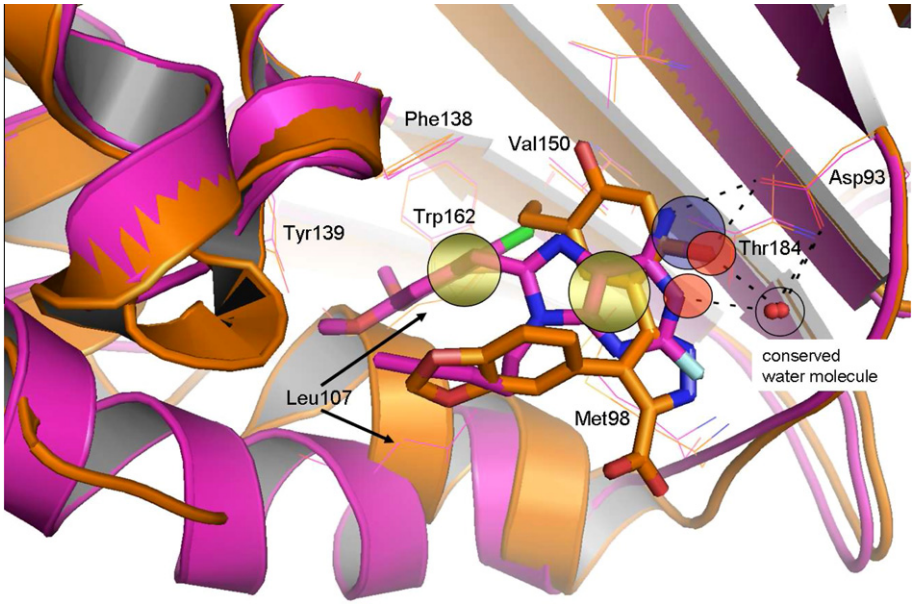

Figure 2. H-bond interactions (dashed lines) of published Hsp90 inhibitors: purine-derivative in 'helical form' (PDB-code 1UYF, magenta) and resorcinol-derivative (PDB-code 1YC1, orange) in 'open form' of Hsp90. Crucial contacts were used as pharmacophore filters (H-donor: blue, H-acceptor: red, lipophilic: golden) for virtual screening by docking.

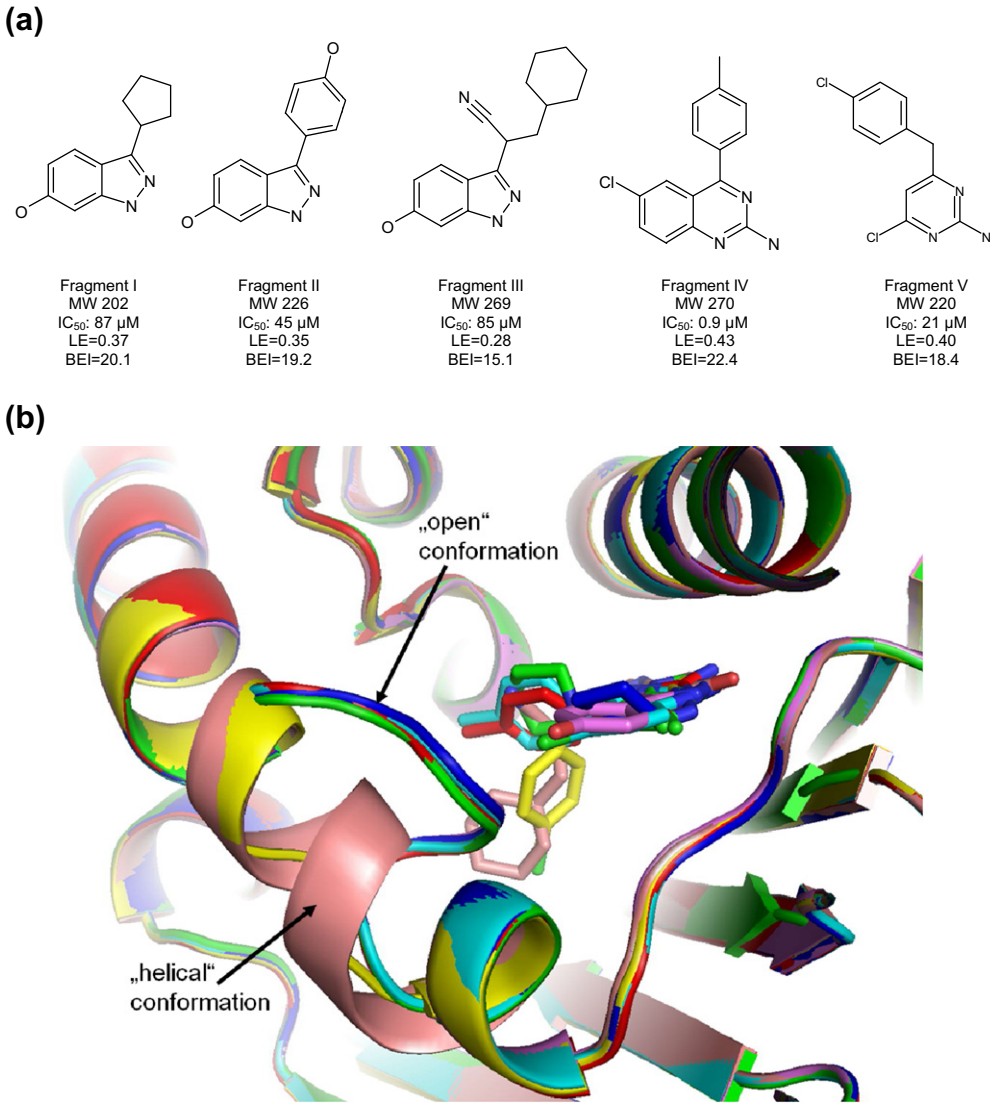

Figure 3. (a) Chemical structures of identified fragment hits with calculated ligand efficiency (LE)[37] and binding efficiency index (BEI).[38] (b) Superimposition of Hsp90 X-ray structures with all 5 fragment hits revealed the helical form for fragments III and V and the open conformation for fragments I, II and IV.

pocket of the helical form. In contrast, this lipophilic pocket is not adressed by fragment II, but its phenole substituent forms π-interactions to Met98 towards the solvent entrance of the ATP-site. This flip in orientation confirms the observation that subtle changes in the chemistry of a fragment can induce a change in compound orientation, which has been reported recently for similar indazole fragments.[18]

The indazole analogs designed to obtain structure–activity relationships were synthesized by following the synthetic sequences summarized in Schemes 1 and 2. Thus, compounds **4a**–**z** were obtained from 2-hydroxy-4-fluoro-benzoic acid **1a**, which was esterified with methyl iodide in dimethylformamide and subsequently Friedl–Crafts acylated at position 5 with phenylacetyl chloride at 0 °C to give **2a**. Cyclization of **2a** with hydrazine in dioxane afforded the key intermediate **3a**. After saponification of methyl ester **3a** to the corresponding acid, the final indazole carboxamides **4a**–**z** were assembled using either amide coupling chemistry or activation via the acyl chloride.[27,28] Compounds with a substituent at the benzyl moiety were not accessible via this protocol, because the Friedl–Crafts acylation with substituted phenylacetyl chlorides failed. Only compound **24** bearing a methoxy group at the 3-position of the benzyl residue could be obtained through acylation with 3-nitrophenylacetyl chloride followed by the conversion of the nitro group of **2b** via a reduction/diazotization/substitution protocol to gain compound **2c**. Cyclization to **3b** and subsequent formation of the benzyl-methyl-amide **24** were performed as described for compounds **4**.

For all other 3-benzyl derivatives (**12**, **19**–**23**, **25**–**28**) and the 3-phenethyl derivative **29** an alternative synthesis route was established as depicted in Scheme 2. 2-Bromo-5-fluoro-anisole turned out to be the reagent of choice, because its increased reactivity for Friedl–Crafts acylations allowed the conversion to the corresponding ketones **6** at low temperature (−50 °C) at which side reactions of the acyl halide could be avoided. Only the synthesis of ketone **7**, precursor of the 3-phenethyl derivative **29**, by acylation with 3-phenyl-propionyl chloride remained difficult due to the preferred intramolecular cyclization to indane-1-one. Formation of the indazole core by cyclization of **6** and **7** with hydrazine in dioxane afforded compounds **8** and **9**. These compounds were key intermediates for the preparation of the methoxy-substituted derivative **12**, the hydroxyl-indazoles **19**–**23** and **25**–**29**, respectively. Compound **12** was obtained from **8** via palladium-catalyzed methoxy-carbonylation using $Pd(dppf)_2Cl_2 \cdot CH_2Cl_2$ as catalyst followed by saponification of the ester **10** to the corresponding acid

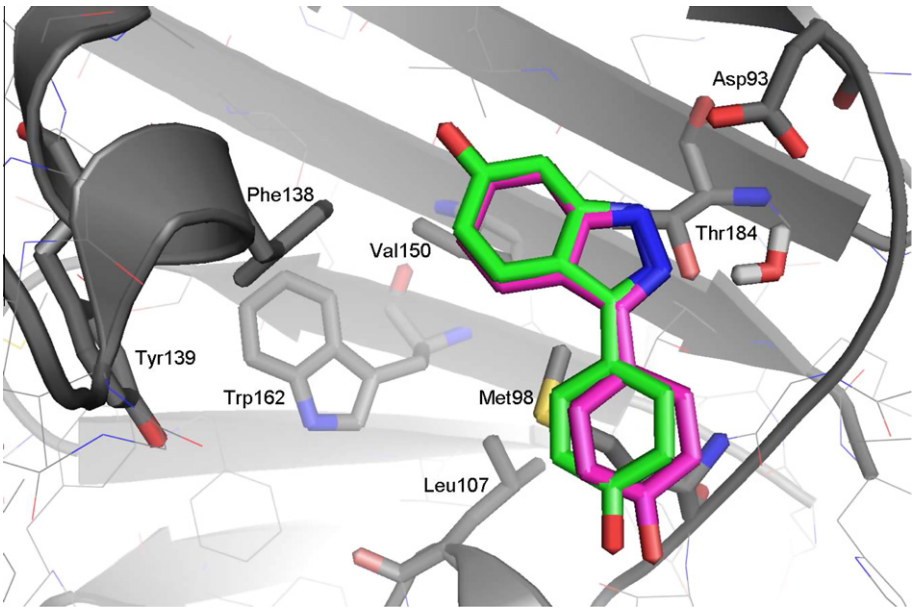

Figure 4. X-ray structure of fragment II in complex with Hsp90 (magenta, PDB-code: 4EEH, PDB deposition number: RCSB071515, resolution 1.60 Å, R_{work}/R_{free} 0.185/0.212) in comparison with the best docking solution (green).

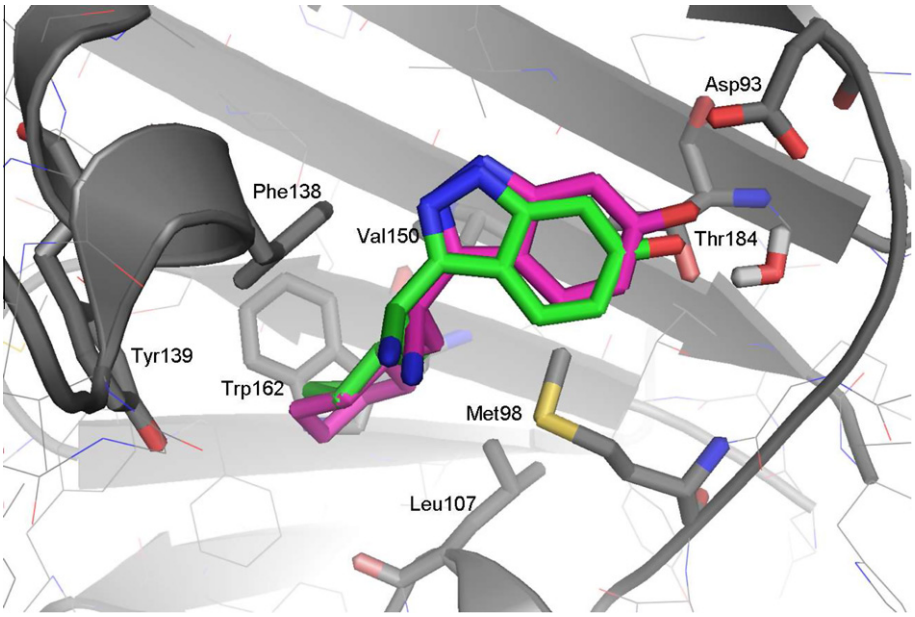

Figure 5. X-ray structure of fragment III in complex with Hsp90 (magenta, PDB-code: 4EFT, PDB deposition number: RCSB071563, resolution 2.12 Å, R_{work}/R_{free} 0.206/0.230) in comparison with the best docking solution (green).

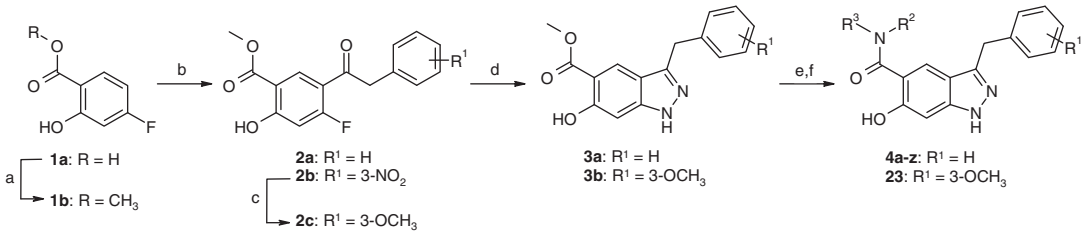

Scheme 1. Reagents and conditions: (a) $KHCO_3$, CH_3I, DMF, 40 °C, 3 h; (b) (i) R^1-$PhCH_2COCl$, $AlCl_3$, CH_2Cl_2, 0 °C→rt, over night; (ii) 1 N HCl, 0 °C; (c) (i) H_2/Raney-Ni, THF, rt, 3 h; (ii) nitrosonium tetrafluoroborate, ACN, 0 °C, 2.5 h; (iii) CF_3COOH, MeOH, 60 °C, 1 h; (d) $(NH_2)_2{\cdot}H_2O$, dioxane, reflux, 1–3 h; (e) NaOH, dioxane, reflux, 1 h; (f) R^2R^3NH, EDCI·HCl, HOBt·H_2O, DIPEA, DMF, rt, over night; or (i) $SOCl_2$, THF, rt; (ii) R^2R^3NH, DIPEA, THF, rt, 1–3 h.

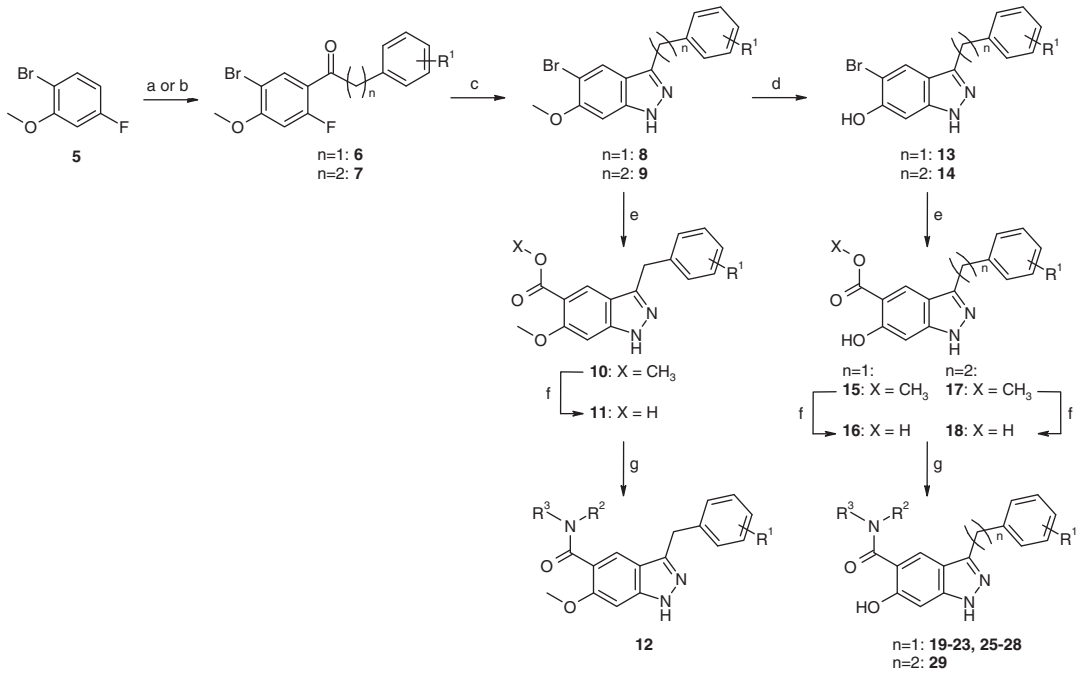

Scheme 2. Reagents and conditions: (a) (i) R^1-$PhCH_2COCl$, $AlCl_3$, CH_2Cl_2, −50→−10 °C–rt, 1–16 h; (ii) 1 N HCl, 0 °C; (b) (i) $Ph(CH_2)_2COCl$, $AlCl_3$, CH_2Cl_2, −55→−40 °C, 30 min; (ii) 1 N HCl, 0 °C; (c) $(NH_2)_2{\cdot}H_2O$, dioxane, reflux, 1.5–3 h; (d) BBr_3, CH_2Cl_2, rt, 16–60 h; (e) $Pd(dppf)_2Cl_2{\cdot}CH_2Cl_2$, 4 bar CO, Et_3N, MeOH/toluene, 100 °C, over night; (f) NaOH, dioxane, reflux, 1 h; (g) (i) $SOCl_2$, THF, rt; (ii) R^2R^3NH, DIPEA, THF, rt, 1 h.

11 and formation of the final amide **12**. Attempts to directly get intermediates **16** from compounds **10** via cleavage of the ester and methoxy group at once under acidic conditions failed. For this reason, we established an alternative protocol for the preparation of derivatives **19**–**23** and **25**–**29**. Cleavage of the methylether of compounds **8** and **9** with boron tribromide in dichloromethane afforded the hydroxyl-indazols **13** and **14**, which were further derivatized using the established reaction sequence for compound **12**.[27,29]

Information gained from X-ray structures of each of the indazole fragments and other in-house Hsp90 inhibitors was used to drive the fragment evolution process. Since both the NH as well as the OH group forms hydrogen bonds to Asp93 and a network of conserved water molecules, we expected them to be pivotal for the binding mode and therefore these structural features were retained. A ligand-induced lipophilic pocket was observed in the helical form of Hsp90 upon binding of purine derivatives[22,23] or our in-house resorcinols, which bear substituted amides in the *ortho*-position of one hydroxyl group.[30] Based on the bioisosteric relationship of indazoles and phenols, which has been exemplified for other targets,[31–33] we expected that substituted amides adjacent to the hydroxyl group would address this lipophilic pocket. Thus, we focused on the modification at two positions of the indazole core to gain SAR.

Comparison of the activities of the initial fragments and compound **4a** in the Hsp90 binding assay revealed that an amide residue in *ortho* position of the hydroxy group is tolerated, in principal. Furthermore, introduction of tertiary amides showed a tractable enhancement of activity in the Hsp90 binding assay (**4b**–**4f**, Table 1). Compounds **4b**, **4c** with *n*-alkyl chains have an activity in the single-digit μM range, which is a 45-fold improvement in potency compared to fragment III. We expected a furanyl residue to further enhance potency by forming additional contacts as observed for PU derivatives. Indeed, for compound **4f** an IC_{50} of 610 nM was found, however this derivative was less potent in the viability assay[26] with A2780 cells than compound **4e** bearing a methyl-benzyl group at the amide nitrogen. Interestingly, the 3-phenethyl derivative **29**, which is a close analog of the initial fragment III, is very potent in the Hsp90 binding assay (IC_{50} = 230 nM). However, this compound was also less potent (about fivefold) in the viability assay. Thus, we kept the benzyl residue at the 3-position and further investigated the amide SAR.

Our initial variation clearly revealed a methyl-benzyl group (**4e**) as most favorable amide substituent. Thus, we kept this moiety and explored its substitution pattern with a diverse set of substituents in the *ortho*-, *meta*- and *para* position (Table 2). Although we could improve the biochemical potency for some derivatives such as **4s**, **4v** or **4x**, the unsubstituted compound **4e** remained the best compound in the viability assay using A2780 cells with an IC_{50} value of about 1 μM. Based on these data we already surmised that such indazole amides may bind in a reversed orientation compared to the resorcinol-amides.[30] Next, we explored the SAR of the benzyl moiety at the 3-position of the indazole core. These efforts clearly showed that small, lipophilic substituents in the *meta*-position are favorable resulting in several compounds with improved activity in the Hsp90 binding assay and more importantly cellular activity (**22a**, IC_{50} = 0.41 μM; **23b**, IC_{50} = 0.49 μM). For all other analogs (**19–21**, **24–28**) bearing various substituents at different positions of the benzyl ring the binding affinity was more or less unaffected. We also examined the influence of the second substituent at the amide nitrogen. A methyl group (**23b**) represents the optimum at this position, while a partial decrease in activity in the Hsp90 binding assay was observed for compound **23a** (R^2 = H) and **23c** (R^2 = ethyl). We assumed that the methyl residue is required to keep the amide in the right orientation and fits into a narrow sub-pocket at this area of the ATP-site. Interestingly, a total loss of activity still occurred when the hydroxyl group of the optimized compound **23b** was changed from a donor to an acceptor through methylation (**12**).

A real breakthrough for further optimization work was the elucidation of the X-ray structure of compound **23b**, which was solved at 2.0 Å resolution (Fig. 6). This crystal structure revealed

Table 1
Biological data of 6-hydroxy-1*H*-indazole-5-carboxylic acid amide derivatives **4a**–**4f** and **29**

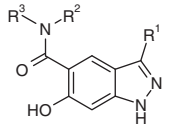

4a-f, 29

Compound	R^1	R^2	R^3	Hsp90 binding assay IC_{50}[a] (μM)	A2780 viability assay IC_{50}[a] (μM)
4a	Bzl	H	H	61	nd
4b	Bzl	CH_3	*n*-C_3H_7	1.9	>10
4c	Bzl	CH_3	*n*-C_4H_9	1.8	7.6
4d	Bzl	CH_3	$(CH_2)_2OCH_3$	4	nd
4e	Bzl	CH_3	Bzl	0.66	0.98
4f	Bzl	CH_3	2-Furanyl	0.61	2.5
29	$(CH_2)_2Ph$	CH_3	Bzl	0.23	4.6

[a] For assay conditions and determination of IC_{50} values see Supplementary data.

Table 2
Summary of biological data of 3-benzyl-6-hydroxy-1*H*-indazole-5-carboxylic acid amide derivatives **4, 12** and **19**–**28**

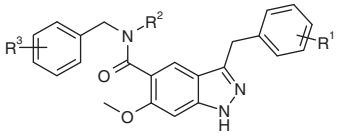

12

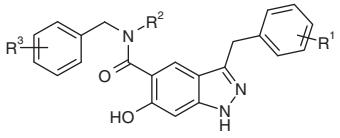

4, 19-28

Compound	R^1	R^2	R^3	Hsp90 binding assay IC_{50}[a] (μM)	A2780 viability assay IC_{50}[a] (μM)
4e	H	CH_3	H	0.66	0.98
4g	H	CH_3	2-F	0.9	1.5
4h	H	CH_3	2-Cl	1.1	1.1
4i	H	CH_3	2-Br	0.61	1.2
4j	H	CH_3	2-CH_3	0.74	4.4
4k	H	CH_3	2-OCH_3	1.7	5.4
4l	H	CH_3	3-F	0.57	5
4m	H	CH_3	3-Cl	1.5	5.3
4n	H	CH_3	3-Br	1.3	7.1
4o	H	CH_3	3-CH_3	3.6	nd
4p	H	CH_3	3-OCH_3	0.98	3.8
4q	H	CH_3	3-CF_3	3.4	nd
4r	H	CH_3	4-F	1.1	4.1
4s	H	CH_3	4-Cl	0.33	2.6
4t	H	CH_3	4-Br	1.1	2.8
4u	H	CH_3	4-CH_3	0.63	6.9
4v	H	CH_3	4-C_2H_5	0.39	9.4
4w	H	CH_3	4-OC_2H_5	0.76	3.2
4x	H	CH_3	2,3-OCH_3	0.47	4.8
4y	H	CH_3	3-OCH_3, 4-Cl	2.3	4.1
4z	H	CH_3	3-F, 4-Cl	0.98	>10
12	3-CH_3	CH_3	H	>20	nd
19	2-Cl	CH_3	H	2.6	nd
20	2-CH_3	CH_3	H	2.4	nd
21	3-F	CH_3	H	1.3	1.7
22a	3-Cl	CH_3	H	0.4	0.41
23a	3-CH_3	H	H	1.5	>10
23b	3-CH_3	CH_3	H	0.25	0.49
23c	3-CH_3	C_2H_5	H	3.0	nd
24	3-OCH_3	CH_3	H	1.4	nd
25	3-C_2H_5	CH_3	H	1.3	nd
26	4-Cl	CH_3	H	5.7	nd
27	4-CH_3	CH_3	H	1.3	>10
28	4-C_2H_5	CH_3	H	2.5	>10

[a] For assay conditions and determination of IC_{50} values see Supplementary data.

that such indazole amides bind according to the orientation of fragment III rather than fragment II. The 3-methylbenzyl substituent is deeply buried in the lipophilic pocket of the helical form with vdW-contacts to Met98, Leu103, Phe138, Val150 and Trp162. The aromatic face on one side of the second benzyl group of **23b** is bent towards the indazole ring with an interplanar angle of ~50° and in lipophilic contact with Leu107. The aromatic face on the rear side is located at the surface of the **23b** complex and oriented towards the solvent, which allows the introduction of diverse residues.

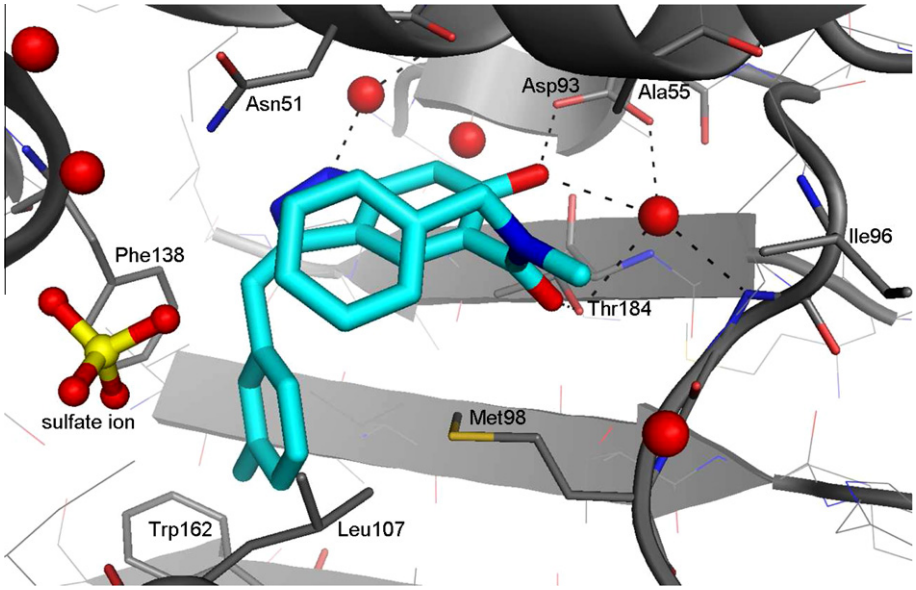

Figure 6. X-ray structure of compound **23b** bound to ATP-site of Hsp90 (PDB-code 4EFU, PDB deposition number: RCSB071564, resolution 2.0 Å, R_{work}/R_{free} 0.204/0.223) with hydrogen bonds shown as dashed lines.

Table 3
Summary of biological data of 3-benzyl-6-hydroxy-1*H*-indazole-5-carboxylic acid amide derivatives **22** and **23**

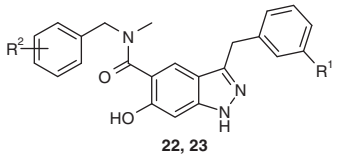

22, 23

Compound	R^1	R^2	Hsp90 binding assay IC_{50} (μM)[a]	A2780 viability assay IC_{50} (μM)[a]
22a	Cl	H	0.4	0.41
22b	Cl	2-Br	0.59	0.13
22c	Cl	3-F	0.71	0.44
22d	Cl	4-F	0.8	0.41
22e	Cl	4-OCH_3	0.8	0.39
22f	Cl	3,4-OCH_3	0.73	2.4
22g	Cl	3-$NHSO_2CH_3$	0.41	3.2
22h	Cl	4-$CH_2NHSO_2CH_3$	0.06	0.57
23b	CH_3	H	0.25	0.49
23d	CH_3	2-Br	0.78	0.31
23e	CH_3	3-F	0.37	0.44
23f	CH_3	4-F	0.58	0.59
23g	CH_3	4-OCH_3	0.46	0.54
23h	CH_3	3-F, 4-Cl	0.17	0.93
23i	CH_3	3-OCH_3, 4-Cl	0.68	1.6
23j	CH_3	3,4-OCH_3	0.58	3.7
23k	CH_3	3,4-F	0.5	0.53
23l	CH_3	3-$NHSO_2CH_3$	0.2	4.0
23m	CH_3	4-$NHSO_2CH_3$	0.35	1.6
23n	CH_3	4-$CH_2NHSO_2CH_3$	0.15	0.71

[a] For assay conditions and determination of IC_{50} values see Supplementary data.

The impact on activity of the substitution at this phenyl ring was subject of the preparation of the next set of compounds. As compounds with a methyl or chloro substituent at the *meta*-position showed the best cellular activity, we adhered to these residues at position R^1 and explored modifications at position R^2. The biological data of these derivatives are reported in Table 3. In general, the SAR for both subseries is fairly similar, but the compounds with the chloro substituent in position R^1 are more potent in the viability assay. Small residues like fluoro or methoxy in *meta* or *para* position are well tolerated (**22c–e, 23e–g**). Introduction of the relatively bulky bromine atom in the *ortho* position (**22b, 23d**) slightly improved the cellular activity. Interestingly, the X-ray structure of compound **23b** indicated the presence of a sulfate ion from the crystallization buffer in the electron density map in ~4 Å distance of the surface exposed benzyl group. This structural information together with molecular modeling studies prompted us to introduce sulfonamide substituents in the *para*-position of the second benzyl group. The resulting 4-methylsulfonamide derivative **22h** (IC_{50} = 59 nM) is >1000-fold more potent than the initial fragment and biochemically the most potent compound in

Table 4
Antiproliferative activities and Hsp70 up-regulation for selected compounds

Compound	Viability assays IC_{50}[a] (μM)				Hsp70 up-regulation IC_{50}[a] (μM)
	A2780	PC-3	MCF-7	Colo-205	A2780
22h	0.57	4.3	3.5	9.5	1
23n	0.71	>10	4.7	3.7	1.1

[a] For assay conditions and determination of IC_{50} values see Supplementary data.

this series. However, as already observed by other groups, this did not translate accordingly to cellular activity.[34–36] Nevertheless, the most potent compounds, **22h** and **23n**, showed reasonable antiproliferative activity in different cancer cell lines and caused the expected up-regulation of Hsp70 in A2780 cells (Table 4).

In conclusion, we have reported the identification of the indazole scaffold for competitively inhibiting the ATP binding site of Hsp90 by a fragment-based approach. Analysis of the X-ray structures of these fragments and other inhibitors bound to Hsp90 allowed the design of compounds with significantly improved potency. Compounds from this series displayed nM activities in the Hsp90 binding assay, inhibited cell proliferation in different human cancer cell lines and caused the expected up-regulation of Hsp70 in A2780 cells. The promising data presented here have prompted further evaluation of this scaffold and that work remains ongoing.

Supplementary data

Supplementary data associated with this article can be found, in the online version, at http://dx.doi.org/10.1016/j.bmcl.2012.04.121. These data include MOL files and InChiKeys of the most important compounds described in this article.

References and notes

1. Young, J. C.; Agashe, V. R.; Siegers, K.; Hartl, F. U. *Nat. Rev. Mol. Cell Biol.* **2004**, *5*, 781.
2. Mosser, D. D.; Morimoto, R. I. *Oncogene* **2004**, *23*, 2907.
3. Whitesell, L.; Lindquist, S. L. *Nat. Rev. Cancer* **2005**, *5*, 761.
4. Maloney, A.; Workman, P. *Expert Opin. Biol. Ther.* **2002**, *2*, 3.
5. Kamal, A.; Boehm, M. F.; Burrows, F. J. *Trends Mol. Med.* **2004**, *10*, 283.
6. Chiosis, G.; Vilenchik, M.; Kim, J.; Solit, D. *Drug Discovery Today* **2004**, *9*, 881.
7. Hanahan, D.; Weinberg, R. A. *Cell* **2000**, *100*, 57.
8. Neckers, L.; Schulte, T. W.; Mimnaugh, E. *Invest. New Drugs* **1999**, *17*, 361.
9. Soga, S.; Shiotsu, Y.; Akinaga, S.; Sharma, S. V. *Curr. Cancer Drug Targets* **2003**, *3*, 359.
10. Banerji, U.; O'Donnell, A.; Scurr, M.; Pacey, S.; Stapleton, S.; Asad, Y.; Simmons, L.; Maloney, A.; Raynaud, F.; Campbell, M.; Walton, M.; Lakhani, S.; Kaye, S.; Workman, P.; Judson, I. J. *Clin. Oncol.* **2005**, *23*, 4152.
11. Wang, Y.; Trepel, J. B.; Neckers, L. M.; Giaccone, G. *Curr. Opin. Invest. Drugs* **2010**, *11*, 1466.
12. Brough, P. A.; Aherne, W.; Barril, X.; Borgognoni, J.; Boxall, K.; Cansfield, J. E.; Cheung, K.-M. J.; Collins, I.; Davies, N. G. M.; Drysdale, M. J.; Dymock, B.; Eccles, S. A.; Finch, H.; Fink, A.; Hayes, A.; Howes, R.; Hubbard, R. E.; James, K.; Jordan, A. M.; Lockie, A.; Martins, V.; Massey, A.; Matthews, T. P.; McDonald, E.; Northfield, C. J.; Pearl, L. H.; Prodromou, C.; Ray, S.; Raynaud, F. I.; Roughley, S. D.; Sharp, S. Y.; Surgenor, A.; Walmsley, D. L.; Webb, P.; Wood, M.; Workman, P.; Wright, L. *J. Med. Chem.* **2008**, *51*, 196.
13. Woodhead, A. J.; Angove, H.; Carr, M. G.; Chessari, G.; Congreve, M.; Coyle, J. E.; Cosme, J.; Graham, B.; Day, P. J.; Downham, R.; Fazal, L.; Feltell, R.; Figueroa, E.; Frederickson, M.; Lewis, J.; McMenamin, R.; Murray, C. W.; O'Brian, M. A.; Parra, L.; Patel, S.; Phillips, T.; Rees, D. C.; Rich, S.; Smith, D.-M.; Trewartha, G.; Vinkovic, M.; Williams, B.; Woolford, A. J.-A. *J. Med. Chem.* **2010**, *53*, 5956.
14. Bao, R.; Lai, C.-J.; Qu, H.; Wang, D.; Yin, L.; Zifcak, B.; Atoyan, R.; Wang, J.; Samson, M.; Forrester, J.; DellaRocca, S.; Xu, G.-X.; Xu, T.; Zhai, H.-X.; Cai, X.; Qian, C. *Clin. Cancer Res.* **2009**, *15*, 4046.
15. Immormino, R. M.; Kang, Y.; Chiosis, G.; Gewirth, D. T. *J. Med. Chem.* **2006**, *49*, 4953.
16. Messaoudi, S.; Peyrat, J.-F.; Brion, J.-D.; Alami, M. *Expert Opin. Ther. Patents* **2011**, *21*, 1501.
17. Foloppe, N. *Future Med. Chem.* **2011**, *3*, 1111.
18. Roughley, S. D.; Hubbard, R. E. *J. Med. Chem.* **2011**, *54*, 3989.
19. Congreve, M.; Carr, R.; Murray, C.; Jhoti, H. *Drug Discovery Today* **2003**, *8*, 876.
20. Barril, X.; Brough, P.; Drysdale, M.; Hubbard, R. E.; Massey, A.; Surgenor, A.; Wright, L. *Bioorg. Med. Chem. Lett.* **2005**, *15*, 5187.
21. Kreusch, A.; Han, S.; Brinker, A.; Zhou, V.; Choi, H. S.; He, Y.; Lesley, S. A.; Caldwell, J.; Gu, X. J. *Bioorg. Med. Chem. Lett.* **2005**, *15*, 1475.
22. Wright, L.; Barril, X.; Dymock, B.; Sheridan, L.; Surgenor, A.; Beswick, M.; Drysdale, M.; Collier, A.; Massey, A.; Davies, N.; Fink, A.; Fromont, C.; Aherne, W.; Boxall, K.; Sharp, S.; Workman, P.; Hubbard, R. E. *Chem. Biol.* **2004**, *11*, 775.
23. Stebbins, C. E.; Russo, A. A.; Schneider, C.; Rosen, N.; Hartl, F. U.; Pavletich, N. P. *Cell* **1997**, *89*, 239.
24. Taldone, T.; Sun, W.; Chiosis, G. *Bioorg. Med. Chem.* **2009**, *15*, 2225.
25. Rarey, M.; Kramer, B.; Lengauer, T.; Klebe, G. *J. Mol. Biol.* **1996**, *261*, 470.
26. For details of the binding assay, the cellular assay, crystallization and structure determination, and virtual screening please see the Supplementary data.
27. Buchstaller, H.-P.; Eggenweiler, H.-M.; Wolf, M.; Sirrenberg, C. WO2008/003396, 2008.
28. *Analytical data (for LC–MS conditions see* Supplementary data*) for a representative compound* ***4e***: ^{1}H NMR (400 MHz, DMSO-d_6, 90 °C) δ (ppm): 12.15 (s, 1H), 9.67 (s, 1H), 7.36–7.10 (m, 11H), 6.82 (s, 1H), 4.53 (s, 2H), 4.17 (s, 2H), 2.76 (s, 3H). LC–MS: R_t = 2.20 min (polar gradient); ESI *m*/*z* 372.8/373.8 $[M+H]^+$.
29. *Analytical data (for LC–MS conditions see* Supplementary data*) for representative compounds* ***22a***: ^{1}H NMR (400 MHz, DMSO-d_6, 90 °C) δ (ppm): 12.25 (s, 1H), 9.75 (s, 1H), 7.44 (s, 1H), 7.39–7.21 (m, 9H), 6.88 (s, 1H), 4.58 (m, 2H), 4.23 (s, 2H), 2.82 (s, 3H). LC–MS: R_t = 1.76 min (regular gradient); ESI *m*/*z* 406.8/407.8/408.7 $[M+H]^+$; **22h**: ^{1}H NMR (400 MHz, DMSO-d_6, 90 °C) δ (ppm): 12.21 (s, 1H), 9.70 (s, 1H), 7.41 (s, 1H), 7.37–7.14 (m, 9H), 6.84 (s, 1H), 4.53 (s, 2H), 4.20 (s, 2H), 4.15 (d, 2H), 2.82 (s, 3H), 2.76 (s, 3H). LC–MS: R_t = 1.43 min (regular gradient); ESI *m*/*z* 513.2/514.2/515.2/516.2 $[M+H]^+$; **23b**: ^{1}H NMR (400 MHz, DMSO-d_6, 90 °C) δ (ppm): 12.14 (s, 1H), 9.67 (s, 1H), 7.37–7.20 (m, 6H), 7.16–6.92 (m, 4H), 6.82 (s, 1H), 4.53 (s, 2H), 4.12 (s, 2H), 2.76 (s, 3H), 2.22 (s, 3H). LC–MS: R_t = 1.72 min (regular gradient); ESI *m*/*z* 386.8/387.8 $[M+H]^+$; **23n**: ^{1}H NMR (400 MHz, DMSO-d_6, 90 °C) δ (ppm): 12.14 (s, 1H), 9.67 (s, 1H), 7.39–7.19 (m, 6H), 7.17–6.93 (m, 4H), 6.82 (s, 1H), 4.52 (s, 2H), 4.19–4.09 (m, 4H), 2.82 (s, 3H), 2.75 (s, 3H), 2.23 (s, 3H). LC–MS: R_t = 1.39 min (regular gradient); ESI *m*/*z* 493.2/494.2 $[M+H]^+$.
30. Eggenweiler, H.-M.; Sirrenberg, C.; Buchstaller, H.-P.; Wolf, M.; Grädler, U.; März, J.; Musil, D.; Hoppe, E.; Zimmermann, A.; Amendt, C. Wegener, A.; Schwartz, H.; Bomke, J. 240th ACS National Meeting, Boston, MA, United States, August 22–26, 2010; 2010; MEDI-505.
31. Boehm, H. J.; Boehringer, M.; Bur, D.; Gmuender, H.; Huber, W.; Klaus, W.; Kostrewa, D.; Kuehne, H.; Luebbers, T.; Meunier-Keller, N.; Mueller, F. *J. Med. Chem.* **2000**, *43*, 2664.
32. Bamborough, P.; Angell, R. M.; Bhamra, I.; Brown, D.; Bull, J.; Christopher, J. A.; Cooper, A. W. J.; Fazal, L. H.; Giordano, I.; Hind, L.; Patel, V. K.; Ranshaw, L. E.; Sims, M. J.; Skone, P. A.; Smith, K. J.; Vickerstaff, E.; Washington, M. *Bioorg. Med. Chem. Lett.* **2007**, *17*, 4363.
33. Folkes, A. J.; Ahmadi, K.; Alderton, W. K.; Alix, S.; Baker, S. J.; Box, G.; Chuckowree, I. S.; Clarke, P. A.; Depledge, P.; Eccles, S. A.; Friedman, L. S.; Hayes, A.; Hancox, T. C.; Kugendradas, A.; Lensun, L.; Moore, P.; Olivero, A. G.; Pang, J.; Patel, S.; Pergl-Wilson, G. H.; Raynaud, F. I.; Robson, A.; Saghir, N.; Salphati, L.; Sohal, S.; Ultsch, M. H.; Valenti, M.; Wallweber, H. J. A.; Wan, N. C.; Wiesmann, C.; Workman, P.; Zhyvoloup, A.; Zvelebil, M. J.; Shuttleworth, S. J. *J. Med. Chem.* **2008**, *51*, 5522.
34. Pratt, W. B.; Toft, D. O. *Exp. Biol. Med. (Maywood)* **2003**, *228*, 111.
35. Pearl, L. H.; Prodromou, C. *Annu. Rev. Biochem.* **2006**, *75*, 271.
36. Barta, T. E.; Veal, J. M.; Rice, J. W.; Partridge, J. M.; Fadden, P. R.; Ma, W.; Jenks, M.; Geng, L.; Hanson, G. J.; Huang, K. H.; Barabasz, A. F.; Foley, B. E.; Otto, J.; Hall, S. E. *Bioorg. Med. Chem. Lett.* **2008**, *18*, 3517.
37. Hopkins, A. L.; Groom, C. R.; Alex, A. *Drug Discovery Today* **2004**, *9*, 430.
38. Abad-Zapatero, C.; Metz, J. T. *Drug Discovery Today* **2005**, *10*, 464.
39. Sadowski, J. *J. Comput. Aided Mol. Des.* **1997**, *11*, 53.
40. SYBYL 8.0, Tripos International, 1699 South Hanley Rd., St. Louis, Missouri, 63144, USA.